INSTITUTE OF PHYSICS PUBLISHING SUPERCONDUCTOR SCIENCE AND TECHNOLOGY

Supercond. Sci. Technol. **19** (2006) 699–702 doi:10.1088/0953-2048/19/8/003

Enhancement of J_C–B properties in $MoSi_2$-doped MgB_2 tapes

Xianping Zhang[1], Yanwei Ma[1,3], Zhaoshun Gao[1], Zhengguang Yu[1], G Nishijima[2] and K Watanabe[2]

[1] Applied Superconductivity Laboratory, Institute of Electrical Engineering, Chinese Academy of Sciences, PO Box 2703, Beijing 100080, People's Republic of China
[2] High Field Laboratory for Superconducting Materials, Institute for Materials Research, Tohoku University, Sendai 980-8577, Japan

E-mail: ywma@mail.iee.ac.cn

Received 20 February 2006, in final form 7 April 2006
Published 26 May 2006
Online at stacks.iop.org/SUST/19/699

Abstract

$MoSi_2$-doped MgB_2 tapes with different doping levels were prepared through the *in situ* powder-in-tube method using Fe as the sheath material. The effect of $MoSi_2$ doping on the MgB_2/Fe tapes was investigated. It was found that the highest J_C value was achieved in the 2.5 at.%-doped samples, more than a factor of 4 higher than the undoped tapes at 4.2 K, 10 T, then further increasing the doping ratio caused a reduction of J_C. Moreover, all doped tapes exhibited improved magnetic field dependence of J_C. The mechanism of J_C enhancement by $MoSi_2$ doping is also discussed.

(Some figures in this article are in colour only in the electronic version)

1. Introduction

MgB_2 has a high superconducting transition temperature (T_C) and does not have a weak-link problem at grain boundaries. The material cost of MgB_2 is lower than that of other superconducting materials, such as Nb-based superconductors and HTS (high T_C superconductivity) cuprates. Therefore, MgB_2 is a promising candidate for engineering applications at temperatures around 20 K. However, J_C of MgB_2 decreases rapidly under magnetic fields compared to those for the Nb-based superconductors. It is generally agreed that improvement of J_C can be achieved in two ways: improvement of the grain connectivity and introduction of the effective pinning centres [1]. In contrast to HTS, MgB_2 has a relatively large coherence length, and this means that the fluxoids can be pinned by relatively larger particles and precipitates. Accordingly, chemical doping seems to be a very promising way to increase the flux pinning ability and B_{irr} in MgB_2 [2]. Many works have been done on the chemical doping/additive to MgB_2 [3–14]. Of all these materials, various silicides, such as WSi_2, $ZrSi_2$ [11], SiO_2, $MgSi_2$ [12], Si_3N_4 [13], SiC, and Si/N/C [14], are very effective in improving the J_C values of *in situ*-processed MgB_2 tapes. This suggests that silicide doping is effective to improve the J_C properties of MgB_2 tapes. Therefore, it is necessary to investigate other silicide doping in order to understand the mechanism of the flux pinning in MgB_2 and eventually realize the widespread application of MgB_2. In this work, we have fabricated $MoSi_2$-doped MgB_2/Fe tapes and investigated the $MoSi_2$ doping effects on the microstructure and J_C of MgB_2.

[3] Author to whom any correspondence should be addressed.

2. Experimental details

MgB_2 tapes were prepared by the *in situ* powder-in-tube (PIT) method. The sheath material chosen for this experiment was commercially available pure Fe. Mg (325 mesh, 99.8%), B (amorphous, 99.99%), and $MoSi_2$ (2–5 μm, 99%) powders were used as the starting materials. Mg and B powders were mixed with the nominal composition of 1:2, the $MoSi_2$ doping levels were 2.5, 5, 10, 15, 20 at.%, respectively. These mixed powders were packed into Fe tubes, and then cold-rolled into tapes. The final size of the tapes was 3.2 mm width and 0.5 mm thickness. Undoped tapes were similarly fabricated for comparative study. These tapes were sintered in flowing high purity Ar at 650 °C for 1 h, which was followed by furnace cooling to room temperature. To study the effects of sintering temperature on $MoSi_2$-doped MgB_2 tapes, samples heated at 750 °C for 1 h were also made.

The phase constitutions and microstructure of the samples were investigated using x-ray diffraction (XRD), energy

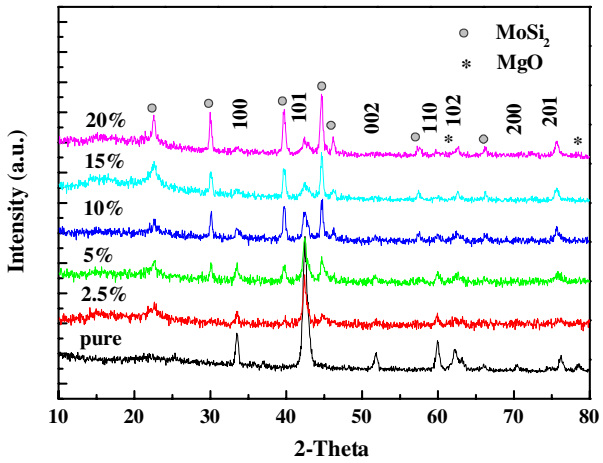

Figure 1. XRD patterns of *in situ* processed undoped and all $MoSi_2$-doped tapes heated at 650 °C for 1 h. The peaks of MgB_2 are indexed, while the peaks of MgO and $MoSi_2$ are marked with asterisks and circles, respectively.

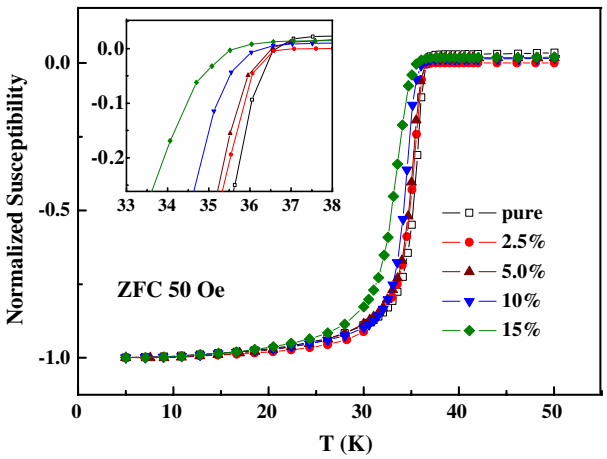

Figure 2. The temperature dependence of the DC magnetic susceptibility curves of the $MoSi_2$-doped and undoped tapes. The inset shows the temperature region close to the superconducting transition.

dispersive x-ray analysis (EDX) and scanning electron microscopy (SEM). For SEM/EDX and XRD analysis, rectangular samples were cut from the tapes, and sheath materials were removed. DC magnetization measurements were performed with a superconducting quantum interference device (SQUID) magnetometer, using small pieces of an MgB_2 layer obtained by removing the sheath material of the samples. The T_C was defined as the onset temperature at which a diamagnetic signal was observed. The transport current I_C at 4.2 K and its magnetic field dependence were evaluated at the High Field Laboratory for Superconducting Materials (HFLSM) at Sendai, by a standard four-probe technique, with a criterion of 1 μV cm^{-1}. Current leads and voltage taps were directly soldered to the sheath material of the tapes. A magnetic field was applied parallel to the tape surface. The critical current density J_C was obtained by dividing I_C by the cross-sectional area of the MgB_2 core.

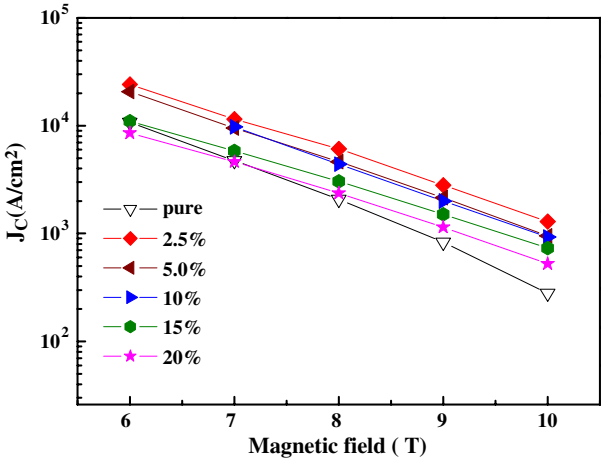

Figure 3. J_C–B properties of Fe-sheathed undoped and $MoSi_2$-doped tapes heated at 650 °C for 1 h.

3. Results and discussion

Figure 1 presents XRD patterns of $MoSi_2$-doped and undoped samples. The XRD pattern for the undoped sample is consistent with the published indices of MgB_2 with a trace amount of MgO. For the 2.5 at.%-doped samples, the $MoSi_2$ phase is clearly seen as one of main impurities along with MgO. $MoSi_2$ phase can be identified in all the doped samples, and its diffraction peaks increase with the increase in doping level. There is no observable shift in the peaks of the XRD patterns. This indicates that there were no changes in the lattice parameters between the undoped and $MoSi_2$-doped samples [15]. It is clear that MgB_2 is inert with respect to $MoSi_2$ at 650 °C. A similar result was also found for WSi_2-doped tapes, as reported by Ma *et al* [11]. On the contrary, the addition of $ZrSi_2$ in MgB_2 tapes resulted in the formation of Zr_3Si_2 and Mg_2Si, no diffraction peaks of the $ZrSi_2$ phase were observed, suggesting that there was a reaction between MgB_2 and $ZrSi_2$ [11]. Since Mo and W elements are in the same element group (VIb), their chemical properties are very close, but Zr element is in the IVb group with a different crystal structure, electron configuration, bonding radius, etc. This may partially explain the different reactivity behaviour of $MoSi_2$ and $ZrSi_2$ in the corresponding doped samples.

The transition temperatures for the doped and undoped samples determined by DC susceptibility measurements are shown in figure 2. T_C obtained as the onset of magnetic screening for the undoped samples was 36.5 K with a transition width of 2 K. For the doped samples, the T_C decreased with increasing doping level and the transition became broad. However, the degree of T_C depression by $MoSi_2$ doping is low, indicating that small substitutions occurred in MgB_2 crystal. T_C for the 2.5% and 5%-doped samples showed little difference, which decreased only 0.5 K compared to the undoped ones, while the T_C for the 15%-doped samples dropped about 2 K with a transition width of 6 K. The broad transition in T_C for the 15%-doped samples may be caused by a large amount of impurities such as $MoSi_2$, and this is in agreement with the XRD patterns in figure 1.

Figure 3 shows the transport J_C at 4.2 K in magnetic fields for the undoped and $MoSi_2$-doped samples heated at

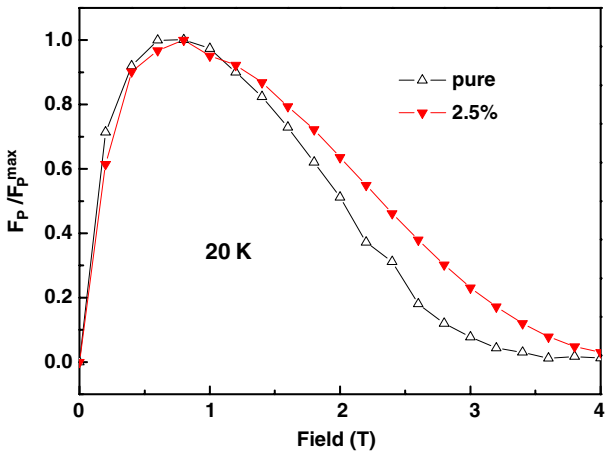

Figure 4. The normalized volume pinning force (F_P/F_P^{max}) versus magnetic field (T) at 20 K for undoped and 2.5% $MoSi_2$-doped tapes heated at 650 °C.

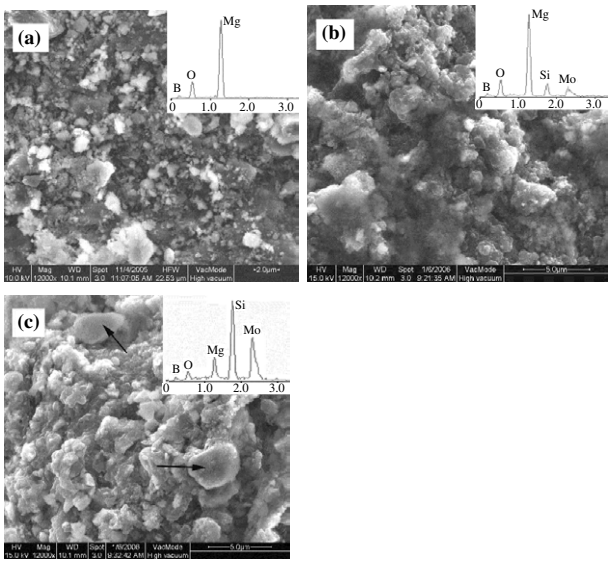

Figure 5. SEM images of the undoped (a), 2.5% (b), and 15% (c) $MoSi_2$-doped samples after peeling off the Fe sheath. Inset: EDX element analysis on the MgB_2 core.

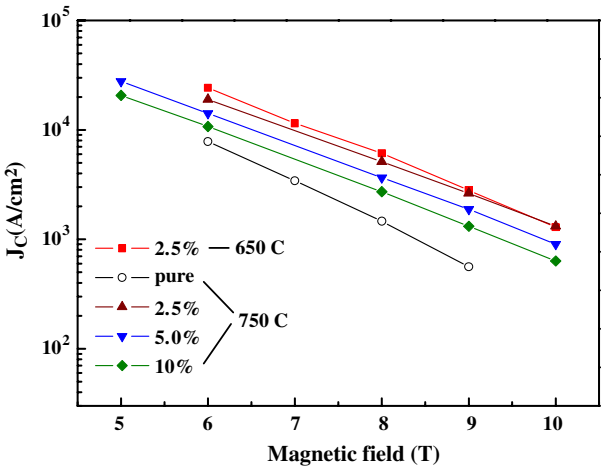

Figure 6. J_C–B properties of Fe-sheathed undoped and $MoSi_2$-doped tapes heated at 750 °C for 1 h. J_C–B curve of 2.5%-doped samples heated at 650 °C was also included.

650 °C. It is noted that the $MoSi_2$ doping enhanced the J_C value in magnetic fields. At 2.5% doping level, the J_C reached 1300 A cm^{-2} at 4.2 K, 10 T, more than a 4-fold improvement compared to the undoped samples, which have a J_C value of about 280 A cm^{-2}. The J_C value of the $MoSi_2$-doped samples decreases with further increases in the doping level. A possible explanation for the decrease of the J_C value with increasing $MoSi_2$ doping level may be due to the large amount of impurities that occurred, which usually lead to weak links at the grain boundaries [2], as will be discussed below. On the other hand, the sensitivity of J_C to magnetic field was reduced by $MoSi_2$ doping, indicating an improved flux pinning ability which is demonstrated in figure 4. Here $F_P(B)$ is obtained from the hysteresis in magnetization curves and is normalized by the maximum volume pinning force F_P^{max} at the same temperature. Although the position of the maximum pinning force shifts only slightly to higher fields for $MoSi_2$-doped samples compared with undoped tapes, the pinning force is clearly larger in the doped tapes, suggesting that pinning centres effective in a high-field region were introduced by $MoSi_2$ doping.

Typical images of the fractured core layers for undoped and doped samples are shown in figure 5. SEM results clearly reveal that the MgB_2 core of the undoped samples was quite loose with some limited melted intergrain regions (see figure 5(a)). However, with the addition of 2.5% $MoSi_2$, the MgB_2 core has a quite uniform microstructure with fewer voids (see figure 5(b)), and consequently the connections between grains are much improved. It should be noted that although the 15%-doped sample is still rather dense according to the SEM image, there are many large particles with a size of 3–5 μm (see figure 5(c)). These large particles had been identified as $MoSi_2$ grains by the EDX analysis. The higher the doping level, the more large particles scatter within the MgB_2 matrix. This is clearly demonstrated by the evident difference in Mo and Si element contents between the 2.5% and 15%-doped samples from the insets of figure 5. Through EDX analysis at randomly selected areas on the MgB_2 core, we found that the $MoSi_2$ ratio is almost identical across the entire sample, suggesting a globally homogeneous phase distribution. As for the 15%-doped samples, these largely dispersed $MoSi_2$ particles, which could decrease the superconducting volume of MgB_2 tapes and weaken the grain linkage, are proposed to be responsible for the reduction of the J_C values.

J_C values versus magnetic field for the 750 °C heat-treated samples are plotted in figure 6. The J_C–B curve of 2.5%-doped samples sintered at 650 °C was also included. Again, it can be seen that the J_C–B properties of the $MoSi_2$-doped samples are improved compared to undoped samples when heated at 750 °C. Like the tapes sintered at 650 °C (see figure 3), the best result was achieved in the 2.5 at.%-doped samples. J_C was degraded by further additions although it was still higher than the undoped sample. In addition, when comparing the 2.5%-doped samples heated at different temperatures, we note that the samples annealed at 750 °C have slightly better field dependence of J_C, implying that a higher sintering temperature

leads to more effective flux pinning centres in the doped samples, thus enhancing flux pinning and improving the high-field J_C.

Clearly, our data for $MoSi_2$-doped tapes showed much better J_C–B performance in the whole range of magnetic fields up to 10 T. Good grain linkage had been thought to be one of the reasons for the high J_C–B properties in doped tapes. However, as proved by several groups [9, 14], the grain linkage improvement alone could not explain the lowered field dependence of J_C in doped tapes, since the grain coupling mainly increases the J_C values, and hardly changes the field dependence of J_C. There must be more effective flux pinning centres in the doped samples than the undoped tapes. Therefore, nanoscale impurity precipitates and/or crystal lattice defects reaction-introduced by $MoSi_2$ doping, serving as strong pinning centres to improve flux pinning as evidenced by figure 4, are the main reason for the excellent J_C–B performance. It should be noted that the size of the $MoSi_2$ particles used was 2–5 μm. In the SiC and C addition, which is significantly effective in increasing J_C in the high-field region, nanometre-sized particles were used [4, 8]. As we know, the surface energy of large particles is much lower than that of nanoscale ones. Thus it is difficult for the micrometre $MoSi_2$ powders to react with Mg or B and to form nanoscale impurities. Therefore, further improvement in J_C–B performance is expected upon use of finer $MoSi_2$ particles.

4. Conclusions

In summary, we have synthesized $MoSi_2$-doped MgB_2 tapes by the *in situ* PIT method. The effect of $MoSi_2$ doping on the microstructures and superconducting properties of MgB_2 tapes has been investigated. It is found that the J_C values have been significantly improved by $MoSi_2$ doping. The best result was achieved for the 2.5 at.% $MoSi_2$ additions. J_C was degraded by further additions. Furthermore, the enhanced field dependence of the $MoSi_2$-doped tapes is due to the pinning by possible segregates or defects caused by the $MoSi_2$ doping.

Acknowledgments

The authors thank Yulei Jiao, Ling Xiao, Xiaohang Li, S Awaji and Liye Xiao for their help and useful discussions. This work is partially supported by the National Science Foundation of China under Grant Nos 50472063 and 50377040 and National '973' Program (Grant No. 2006CB601004).

References

[1] Pachla W, Morawski A, Kovac P, Husek I, Mazur A, Lada T, Diduszko R, Melisek T, Strbık V and Kulczyk M 2006 *Supercond. Sci. Technol.* **19** 1
[2] Flukiger R, Suo H L, Musolino N, Beneduce C, Toulemonde P and Lezza P 2003 *Physica* C **385** 286
[3] Senkowicz B J, Giencke J E, Patnaik S, Eom C B, Hellstrom E E and Larbalestier D C 2005 *Appl. Phys. Lett.* **86** 202502
[4] Ma Y, Zhang X, Nishijima G, Watanabe K, Awaji S and Bai X 2006 *Appl. Phys. Lett.* **88** 072502
[5] Berenov A, Serquis A, Liao X Z, Zhu Y T, Peterson D E, Bugoslavsky Y, Yates K A, Blamire M G, Cohen L F and MacManus-Driscoll J L 2004 *Supercond. Sci. Technol.* **17** 1093
[6] Ueda S, Shimoyama J, Yamamoto A, Horii S and Kishio K 2004 *Supercond. Sci. Technol.* **17** 926
[7] Wang J, Bugoslavsky Y, Berenov A, Cowey L, Caplin A D, Cohen L F, MacManus-Driscoll J L, Cooley L D, Song X and Larbalestier D C 2002 *Appl. Phys. Lett.* **81** 2026
[8] Ma Y *et al* 2006 *Supercond. Sci. Technol.* **19** 133
[9] Sumption M D, Bhatia M, Rindfleisch M, Tomsic M, Soltannian S, Dou S X and Collings E W 2005 *Appl. Phys. Lett.* **86** 092507
[10] Fu B Q *et al* 2002 *J. Appl. Phys.* **92** 73
[11] Ma Y, Kumakura H, Matsumoto A and Togano K 2003 *Appl. Phys. Lett.* **83** 1181
[12] Matsumoto A, Kumakura H, Kitaguchi H and Hatakeyama H 2004 *Supercond. Sci. Technol.* **17** S319
[13] Jiang C H, Nakane T and Kumakura H 2005 *Supercond. Sci. Technol.* **18** 902
[14] Zhang X, Ma Y, Gao Z, Yu Z, Nishijima G and Watanabe K 2006 *Supercond. Sci. Technol.* **19** 479
[15] Li S, White T, Sun C Q, Fu Y Q, Plevert J and Lauren K 2004 *J. Phys. Chem.* B **108** 16415